# CHAPTER II

THEORETICAL BACKGROUND AND LITERATURE REVIEW

2.1 Polyoxymethylene: Crystal Morphology and Molecular Conformation

The (9/5) helical structure was first proposed by Tadokoro *et. al.* (1960) for the molecular conformation of POM to be hexagonal with a unit cell parameters $a = 4.47$Å and $c = 17.39$Å (Figure 2.1). Later, a more accurate (29/16) helical structure was proposed from the layer line intervals by Carazzolo (1960). There are no fundamental differences between those models except for the unit cell parameter c in the latter case is 56.02Å. Crystal morphology structure of the crystalline phase is generally classified into two types; an extended-chain crystal (ECC) and a folded-chain or lamellar crystal (FCC), as shown in Figure 2.2 (a) and (b), depending on sample preparations (Kobayashi *et. al.* 1992). Kobayashi *et. al.* (1992) clarified the definition of the ECC and FCC in the view of geometric term, i.e. R/H, in which $R=R'\rho_r$ and $H=H'\rho_h$. The R'/H' is a parameter describing crystal morphology (the radius to height ratio of a cylindrical crystal, Figure 2.2 (c)) and the ρ_r/ρ_h relates to the shape and size of the polymer chain. The limit of $R/H \rightarrow 0$ corresponds to the extreme case of the extended-chain crystal (ECC) where the dimension as well as the dipole density is far greater in the direction of the chain axis compared with those of the lateral direction. As the ratio R/H increases, approaching infinity, the folded-chain crystal (FCC) is denoted.
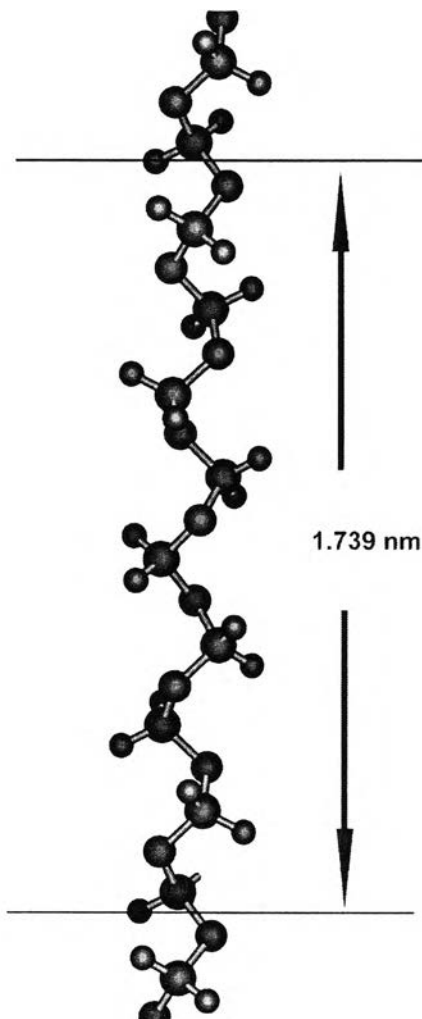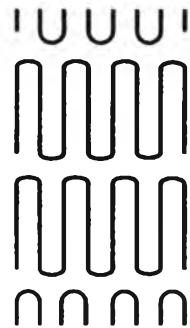
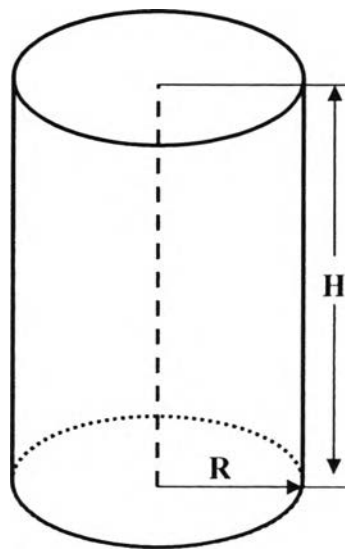**Figure 2.1** Chain conformation of polyoxymethylene.(Todokoro *et al.* 1960)

ECC

(a)
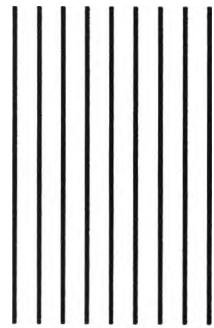
FCC

(b)

(c)

Figure 2.2 Schematic representation of (a) FCC, (b) ECC, and (c) model of cylindrical crystal.(Kobayashi *et al.* 1992)

When polyethylene (PE) is crystallized from the dilute solution, FCC is developed in a form of lamellar crystal (Reneker *et. al.* 1960, Holland *et. al.* 1962) whereas the ECC is obtained by the crystallization under high temperature and high pressure conditions (Wunderlich et. al. 1967, 1968). In the case of POM, the typical FCC is achieved by crystallization from dilute bromobenzene solutions, generating hexagon-shaped lamellar crystals with thickness of about 10 nm, where the molecular chains are folded at the lamellar surface with the stems aligning normal to the surface (Bassett *et. al.* 1964). The typical ECC is achieved through a heterogeneous cationic polymerization of trioxane, giving micron-sized needlelike single crystals where the extended POM molecules align parallel to the needle axis (Todokoro *et. al.* 1963, Carter *et. al.* 1966). The crystal morphology in the melt-grown bulk samples situates in between the FCC and ECC. Moreover, the ECC can be developed on the drawing of the sample (Kobayashi *et. al.* 1992). This crystal morphology is important to control the mechanical properties of the POM.

2.2 Specific Properties for Potential Applications

Development of POM is important not only because of its exceptional balance of machining characteristics, tensile properties (~76 MPa ultimate at 23°C), shear strength, stiffness, toughness, and thermal properties, but also because POM was reported about the biocompatibility (Fister *et. al.* 1985). POM performs good impact strength, low friction, good electrical insulator, wear-resistant, dimensional stability, and chemical resistance. POM shows the melting point at around 175°C, which is above usual steam autoclave temperature. POM is resistant to intermittent high temperatures and it retains its shape and physical integrity at elevated temperatures. POM also has negligible porosity, low moisture absorption (0.9% at saturation), and is deemed safe for food contact use (FDA 21CFR177.2480). The low moisture absorption also results in excellent dimensional stability for close-tolerance machined parts in an aqueous environment.

Laluppa et. al. (1997) studied *in vitro* expansion of hematopoietic progenitor cells by using various plastics. They concluded that POM inhibited both

colony formation and growth of hematopoietic stem cells, whether it was in direct contact with the cells or in indirect contact by conditioning the media. They suggested leaching of toxic compounds from the plastic material as the likely mechanism for these effects. However, POM also has a long history of use in animal studies and as a long-term implant material in a variety of medical applications. These include cardiac valve prostheses (e.g., the Björk-Shiley valve tilting- disk style prosthesis), dental implants (MacAfee *et. al.* 1992) and prosthetics (Dental-D), and orthopedic implants (Brown *et. al.* 1978, Fister *et. al.* 1985) or joint replacement components (Fister *et. al.* 1985). POM performed well in these roles, except as a load-bearing material in total joint replacement where it exhibited excessive wear (Havelin *et. al.* 1986). As a result, its use has decreased, and it has been replaced by materials with better long-term wear and mechanical properties.

In general, the mechanical properties can be improved by blending or initiating the nucleation, etc. Kern and Cherdron (1960) investigated the degradation behavior of POM in the early 1960s to find that the unzipping reaction occurred generated the formaldehyde as a product. The copolymer was proposed to retard the degradation.

The hybridization with inorganic fillers, especially organoclay, to form nanocomposites is another approach to improve the properties of POM from the nano-scale structure. Changing bulk polymer to a fine fiber product may also make it possible for the POM to be used in many advanced applications.

2.3 Polymer/Clay Nanocomposites

2.3.1 General Aspect

In polymer clay nanocomposites (PCN), few wt% of each silicate layer of clay mineral is randomly and homogeneously dispersed on a molecular level in the polymer matrix. After molding to products, it was found that the mechanical, thermal and barrier properties of these products are superior to pristine polymers and/or conventional composite products. The PCN was a new concept proposed by Toyota Central R&D Labs, Inc. (Toyota) which later on was expanded to cover wide

range of polymeric materials. The studies on preparation, structure and interfaces in details lead to novel applications in automotive, electrical and food industries. Passenger cars furnished with a PCN part were launched in 1989 after 4 years of PCN studies. Since then, extensive worldwide researches on PCN have been conducted not only in the industrial sectors but also in the research organizations. The many of international conferences on PCN are conducted every year, and papers on PCN in major journals exceeded 500 in 2005 (Thomson's Web of Science (WOS) showing how PCN is in an exciting research area with promising applications.

The major use of polymers is in molded products. For conventional composites, polymers are successfully reinforced by fiber glass, talc, calcium carbonate, carbon black and other inorganic fillers. The content of the filler is usually between 20 and 40 wt% of a composite, and sometimes exceeds 50 wt% in thermosetting resins. Polymers and fillers are not homogeneously mixed on a microscopic level, and are composed of different phases. The interface is not large, and interaction between the polymer (matrix) and the filler is limited. Takayanagi et. al. (1980) proposed the concept of a molecular composite, on the basis that if the filler is of molecular size, mechanical properties could be further improved, and showed an example of a nylon matrix containing aramide fiber whose content was 5 wt% and diameter was 30 nm. If platelets of nm dimensions were used instead of fibers, the contact surface would become much larger. Smectite clay minerals, especially montmorillonite (MMT), are potential candidates for platelet-type filler for molecular composites, since they are composed of several layers of silicates. These silicates are 1 nm thick and have a cross-sectional area of 100 nm^2, which is very small compared to conventional fillers and also aramide fibers. MMT is the most common and ubiquitous clay mineral, and it is well known that it undergoes intercalation and swelling in the presence of water and organic cations (H. van Olphen, 1977). Syntheses of polymers in the presence of MMT have previously been reported (H. Z. Friedlander 1964, A. Blumstein 1960) but their major component was clay, and these studies were not intended to improve polymers but rather to focus scientific interest. In 1975 Fujiwara et. al. (Unitika Ltd.) tried to prepare a polymer composite with nylon 6 and MMT to make reinforced nylon 6. However, they obtained composites in which the major component was ceramic, as in earlier studies.

These early materials were merely ceramic-like powders, incapable of being injection-molded and therefore practically impossible to process. An impractical molding might be possible, but even if barely molded, the test piece had low tensile strength, brittleness, a very rough surface and a heavy weight; therefore, they cannot be called "polymeric materials."

On the other hand, if the silicates are dispersed randomly and homogeneously in the polymer matrix, the interface area is enormous and a large interaction could be expected. If the silicates are in such a state, interactions between them must be avoided. The shape of silicates is irregular. They are assumed to be square to simplify the problem. As silicates are known about its dimension, 1x100x100 nm^3 and all edges adjoin, the upper limit of their content for nanocomposites is 3.5 vol% (corresponding to 7.5 wt%). If only all apexes of the squares touch, the upper limit of the silicate content is 1.5 vol% (3.8 wt%). It was convinced that the upper limit of clay content is few wt% for PCN. A small amount of clay has been proven to be a key factor for nanocomposites. Actually, it was discovered that when the clay content was less than 5. wt%, such a molecular composite, hybrid or nanocomposite could be obtained. PCN is classified into the "intercalated" type, where the structure of the clay is maintained to some extent, and the "exfoliated" type, where silicate is randomly and homogeneously dispersed. The latter has been focused due to the former may be considered a conventional composite in many cases. The structure of MMT is shown in Figure 2.3, and scanning electron microscopy (SEM) photographs of glass fiber and clay in the polymer matrix are shown in Figure 2.4, where the scales of two photos differ by 100 times.
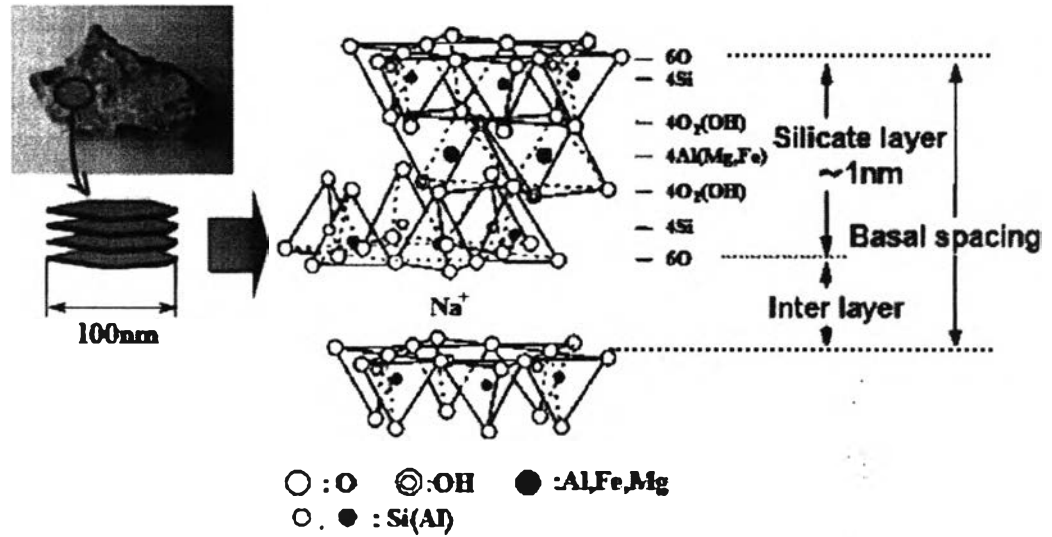
Figure 2.3. Structure of montmorillonite (MMT). (Akane Okada *et al*, 2006).
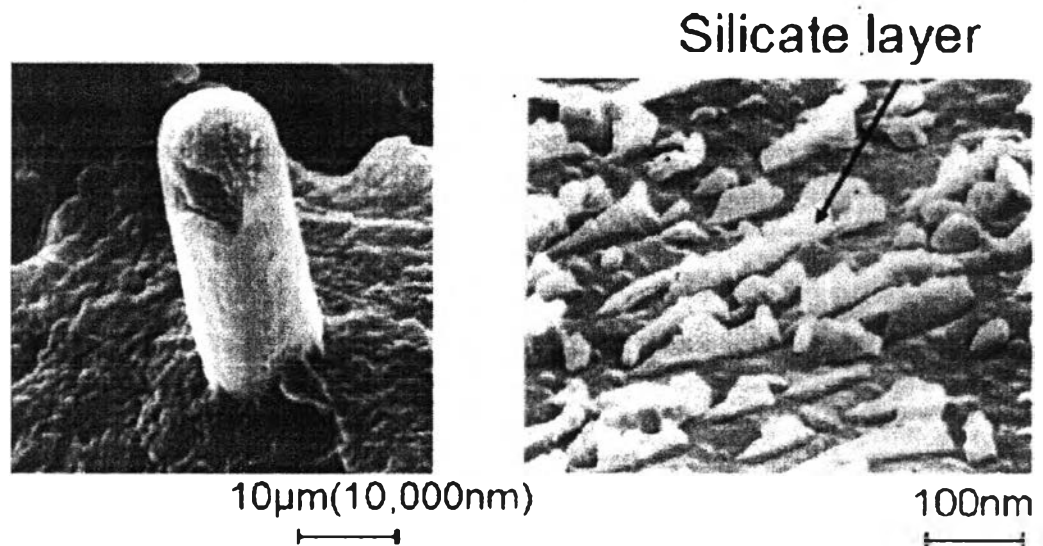
Figure 2.4. Comparison of the size of glass fiber (left) and montmorillonite (right). (Akane Okada *et al*. 2006).

2.3.2 Types of Polymer/Clay Nanocomposites

In general, layered silicates have layer thickness on the order of 1 nm and a very high aspect ratio (e.g. 10–1000). A few weight percent of layered silicates that are properly dispersed throughout the polymer matrix thus create much higher surface area for polymer/filler interaction as compared to conventional composites. Depending on the strength of interfacial interactions between the polymer matrix and layered silicate (modified or not), three different types of PLS nanocomposites are thermodynamically achievable (see Figure 2.5):

a. Intercalated nanocomposites: for intercalated nanocomposites, the insertion of a polymer matrix into the layered silicate structure occurs in a crystallographically regular fashion, regardless of the clay to polymer ratio. Intercalated nanocomposites are normally interlayer by a few molecular layers of polymer. Properties of the composites typically resemble those of ceramic materials.

b. Flocculated nanocomposites: conceptually this is same as intercalated nanocomposites. However, silicate layers are some times flocculated due to hydroxylated edge–edge interaction of the silicate layers.

c. Exfoliated nanocomposites: in an exfoliated nanocomposite, the individual clay layers are separated in a continuous polymer matrix by an average distances that depends on clay loading. Usually, the clay content of an exfoliated nanocomposite is much lower than that of an intercalated nanocomposite.

Generally, the structure of nanocomposites has typically been established using WAXD analysis and transmission electron micrographic (TEM) observation. Due to its easiness and availability WAXD is most commonly used to probe the nanocomposite structure and occasionally to study the kinetics of the polymer melt intercalation (Vaia RA et. al. 1996). By monitoring the position, shape, and intensity of the basal reflections from the distributed silicate layers, the nanocomposite structure (intercalated or exfoliated) may be identified. For example, as shown in Figure 2.6, in an exfoliated nanocomposite, the extensive layer separation associated with the delamination of the original silicate layers in the polymer matrix results in the eventual disappearance of any coherent X-ray diffraction from the distributed silicate layers. On the other hand, for intercalated nanocomposites, the finite layer

expansion associated with the polymer intercalation results in the appearance of a new basal reflection corresponding to the larger gallery height. Although WAXD offers a convenient method to determine the interlayer spacing of the silicate layers in the original layered silicates and in the intercalated nanocomposites (within 1–4 nm), little can be said about the spatial distribution of the silicate layers or any structural non-homogeneities in nanocomposites. Additionally, some layered silicates initially do not exhibit well-defined basal reflections. Thus, peak broadening and intensity decreasing are very difficult to study systematically. Therefore, conclusions concerning the mechanism of nanocomposites formation and their structure based solely on WAXD patterns are only tentative. On the other hand, TEM allows a qualitative understanding of the internal structure, spatial distribution of the various phases, and views of the defect structure through direct visualization. The WAXD patterns and corresponding TEM images of three different types of nanocomposites are presented in Figure 2.6.
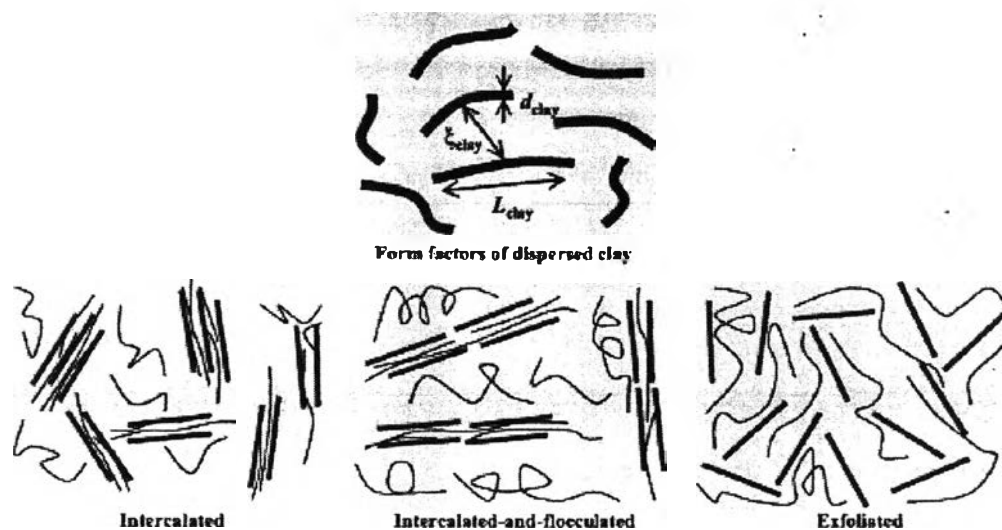
Figure 2.5. Schematically illustration of three different types of thermodynamically achievable polymer/layered silicate nanocomposites. (Sinha Ray S. Okamoto K. and Okamoto M. 2003).
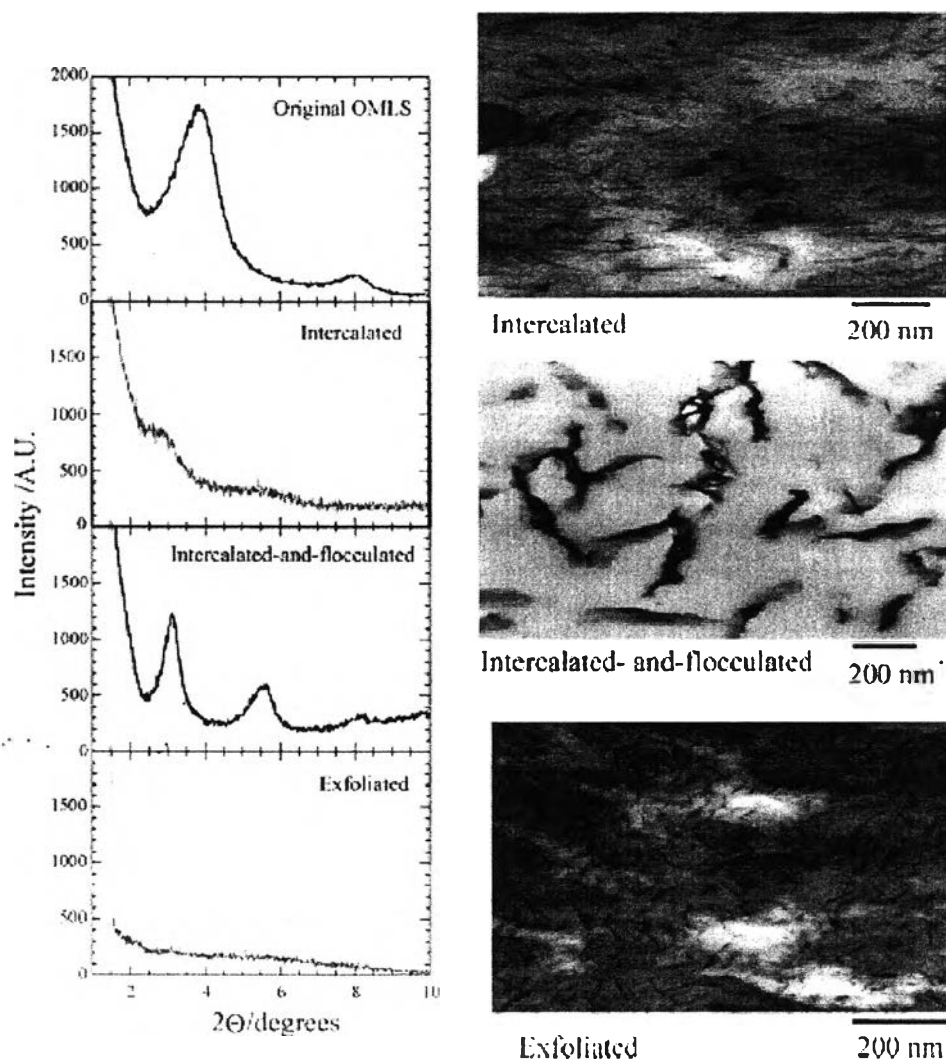
Figure 2.6. WAXD patterns and TEM images of three different types of nanocomposites. (S. Sinha Ray, M. Okamoto, 2003)

2.4 Polyoxymethylene/Clay Nanocomposites

Polyoxymethylene/clay nanocomposites are rarely proposed, which might be due to the difficulty in modifying the POM structure to achieve the intercalation into the clay galleries. The development of POM/clay nanocomposites might bring about properties to overcome the limitations of POM, specifically its low impact toughness, low heat distortion temperature, and to improve its gas barrier property. Previously, W. XU *et. al.* (2001) studied the nonisothermal crystallization kinetics of POM/montmorillonite (MMT) in which the crystallization rate was found to be faster

than that of the neat POM at a given cooling rate. However, the structures and properties of the POM/clay nanocomposites have not yet been elucidated. Pielichowski K. *et. al.* (2006) reported the preparation and characterization of POM-MMT based nancomposites. The mixed tactoid-exfoliated structure was suggested and the mechanical properties were reported to be improved with the incorporation of organo-modified MMT.
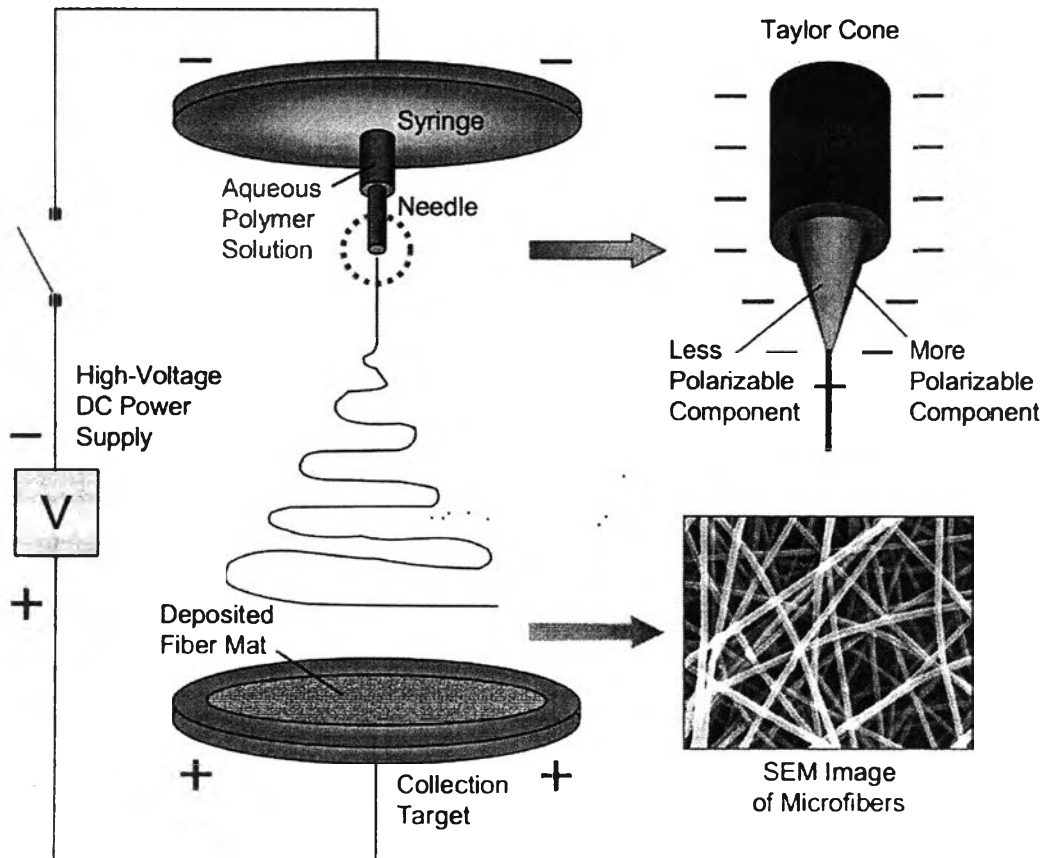
2.5 Electrospinning

Although the term "electrospinning", derived from "electrostatic spinning", was used relatively recently (in around 1994), its fundamental idea dates back more than 60 years earlier. From 1934 to 1944, Formalas published a series of patents, describing an experimental setup for the production of polymer filaments using an electrostatic force. A polymer solution, such as cellulose acetate, was introduced into the electric field. The polymer filaments were formed, from the solution, between two electrodes bearing electrical charges of opposite polarity. One of the electrodes was placed into the solution and the other onto a collector. Once ejected out of a metal spinneret with a small hole, the charged solution jets evaporated to become fibers which were collected on the collector. The potential difference depends on the properties of the spinning solution, such as polymer molecular weight and viscosity. When the distance between the spinneret and the collecting device was short, spun fibers tended to stick to the collecting device as well as to each other, due to incomplete solvent evaporation. Since 1980, the electrospinning process, essentially similar to that described by Baumgarten (1971), has regained much attention which may be the material due in part to a surging interest in nanotechnology, especially ultrafine fibers or fibrous structures of various polymers with diameters down to submicrons or nanometers can be easily fabricated with this process.

2.5.1 Fundamental Aspect

A schematic diagram to interpret electrospinning of polymer nanofibers is shown in Figure 2.7. Basically, there are three components to fulfill the process: a high voltage supplier, a capillary tube with a pipette or needle of small diameter, and a metal collecting screen. In the electrospinning process, a high voltage is used to create an electrically charged jet of polymer solution or melt out of the pipette. Before reaching the collecting screen, the solution jet evaporates or solidifies, and is collected as an interconnected web of small fibers (Deitzel JM et. al. 2001, Reneker DH 2001). One electrode is placed into the spinning solution/melt and the other attached to the collector. In most cases, the collector is simply grounded, as indicated in Figure 2.7. The electric field is subjected to the end of the capillary tube that contains the solution fluid held by its surface tension. This induces a charge on the surface of the liquid. Mutual charge repulsion and the contraction of the surface charges to the counter electrode cause a force directly opposite to the surface tension (Reneker 1997). As the intensity of the electric field is increased, the hemispherical surface of the fluid at the tip of the capillary tube elongates to form a conical shape known as the Taylor cone (Taylor GI 1969). Further increasing the electric field, a critical value is attained with which the repulsive electrostatic force overcomes the surface tension and the charged jet of the fluid is ejected from the tip of the Taylor cone. The discharged polymer solution jet undergoes an instability and elongation process, which allows the jet to become very long and thin. Meanwhile, the solvent evaporates, leaving behind a charged polymer fiber. In the case of the melt the discharged jet solidifies when it travels in the air.

The bending instability of the polymer jet has been explained by Reneker and Yarin (Yarin and Reneker 2008). The typical path of the jet was a straight segment followed by a coil of increasing diameter. After several turns were formed, a new electrical bending instability formed a smaller coil on a turn of the larger coil. The turns of the smaller coil transformed into an even smaller coil and so forth until the elongation stopped, usually by solidification of the thin jet. As shown in Figure 2-8, the straight segment is red, the first bending coil is yellow, and the

third bending coil is blue. There are three turns (which, when observed singly are sometimes referred to as loops) in the yellow coil.

Figure 2.7. Schematic representative diagram of electrospinning process. (www.nano.mtu.edu)
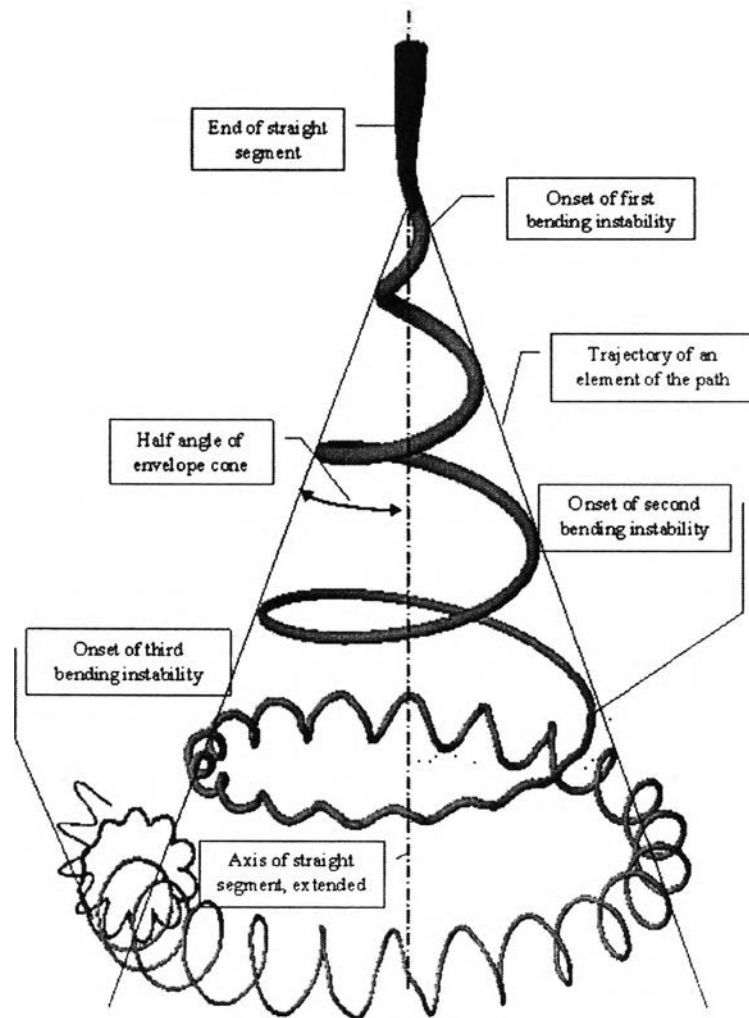
Figure 2.8. Schematic of electrical spinning jet. (Reneker DH, Yarin AL, 2008)

Figure 2.8 shows the prototypical instantaneous position of the path of an electrospinning jet that contains three successive electrical bending instabilities. The straight segment transformed into a three dimensional coil. The jet path continued and transformed to a smaller three dimensional coil, with an axis that followed the curved path extrapolated from the first coil. The second spiral eventually transformed to an even smaller spiral and so forth until the jet solidified, by evaporation of the solvent. At least four successive bending instabilities were observed in some experiments. After the onset of the electrically driven bending instability in electrospinning, every segment of the resulting coil moved outward and downward in a complicated, but not random way. (Reneker DH, Yarin AL, 2008)

2.5.2 Parameter Investigation

Many parameters influence the transformation of polymer solutions into nanofibers through electrospinning. These parameters include (i) the solution properties such as viscosity, elasticity, conductivity, and surface tension, (ii) governing variables such as hydrostatic pressure in the capillary tube, electric potential at the capillary tip, and the gap (distance between the tip and the collecting screen), and (iii) ambient parameters such as solution temperature, humidity, and air velocity in the electrospinning chamber (Doshi and Reneker 1995).

Several researchers investigated spin ability of different polymers. For instance, Fong and Reneker (1999) found for electrospinning of aqueous poly(ethylene oxide) (PEO) dissolved in ethanol-to-water solutions that viscosities in the range of 1–20 poises and surface tension between 35 and 55 dynes/cm were suitable for fiber formation. At viscosities above 20 poises, electrospinning was prohibited because of the instability of flow caused by the high cohesiveness of the solution. Droplets were formed when the viscosity was too low (<1 poise). Similarly, for electrospinning of cellulose acetate (CA) in 2:1 acetone/ DMAc (dimethylacetamide), Liu and Hsieh (2002) recognized that viscosities between 1.2 and 10.2 poises were applicable. Outside that range, the CA solutions could not be electrospun into fibers at room temperature. These two examples clearly demonstrated that the viscosity range of a different polymer solution which is spinnable is different.

As long as a polymer can be electrospun into nanofibers, ideal targets would be in that: (1) the diameters of the fibers are consistent and controllable, (2) the fiber surface is defect-free or defect-controllable, and (3) continuous single nanofibers are collectable. However, researches so far have shown that these three targets are by no means easily achievable.

One of the most important quantities related with electrospinning is the fiber diameter. Since nanofibers are resulted from evaporation or solidification of polymer fluid jets, the fiber diameters will depend primarily on the jet sizes as well as on the polymer contents in the jets. One of the most significant parameters influencing the fiber diameter is the solution viscosity. A higher viscosity results in a larger fiber

diameter. However, when a solid polymer is dissolved in a solvent, the solution viscosity is proportional to the polymer concentration. Thus, the higher the polymer concentration the larger the resulting nanofiber diameters will be. In fact, Deitzel *et. al.* (2001) pointed out that the fiber diameter increased with increasing polymer concentration according to a power law relationship. Demir *et. al.* (2002) further found that the fiber diameter was proportional to the cube of the polymer concentration. Another parameter which affects the fiber diameter to a remarkable extent is the applied electrical voltage. In general, a higher applied voltage ejects more fluid in a jet, resulting in a larger fiber diameter (Demir *et. al.* 2002). It has been found that the polymer concentration also affects the formation of the beads. Fong recognized that higher polymer concentration resulted in fewer beads (Fong and Reneker 1999). In their experiments with PEO polymer, the polymer concentrations of 1–4.5 wt.% were used. The resulting fiber membranes were visualized under SEM, and different fiber morphologies were captured, as shown in Figure 2.9, in which the lowest viscosity, 13 centipoise, corresponded to 1 wt.% PEO concentration, whereas the highest viscosity, 1250 centipoise, corresponded to 4 wt.% concentration. It should be realized that with the 4 wt.% PEO concentration the beads were not reported to completely disappear. Instead, the bead diameters, if any, at higher concentrations were even larger. The shape of the beads changed from spherical to spindlelike when the polymer concentration varied from low to high levels. Doshi & Reneker pointed out that by reducing surface tension of a polymer solution, fibers could be obtained without beads. This might be correct in some sense, but should be applied with caution. It has been recognized by Fong and Liu (1999) that the surface tension seems more likely to be a function of solvent compositions, but is negligibly dependent on the polymer concentration. Different solvents may contribute different surface tensions. However, not necessarily a lower surface tension of a solvent will always be more suitable for electrospinning. Furthermore, adding some filler material into a polymer solution can also result in fibers free of beads. Zong *et. al.* (2002) realized this while electrospinning biodegradable PLDA polymers. They found that with 1 wt.% salt addition, the resulting nanofibers were bead-free. They argued that the addition of salts resulted in a higher charge density on the surface of the solution jet during the electrospinning, bringing more electric

charges to the jet. As the charges carried by the jet increased, higher elongation forces were imposed to the jet under the electrical field, resulting in smaller bead and thinner fiber diameters. This, however, does not imply that a higher applied electrical field could result in fewer beads and smoother nanofibers. In fact, Deitzel *et. al.* investigated the influence of electrical charge, which was applied for electrospinning, on the morphology of PEO nanofibers. They reported that with the increase of the electrical potential the resulting nanofibers became rougher.
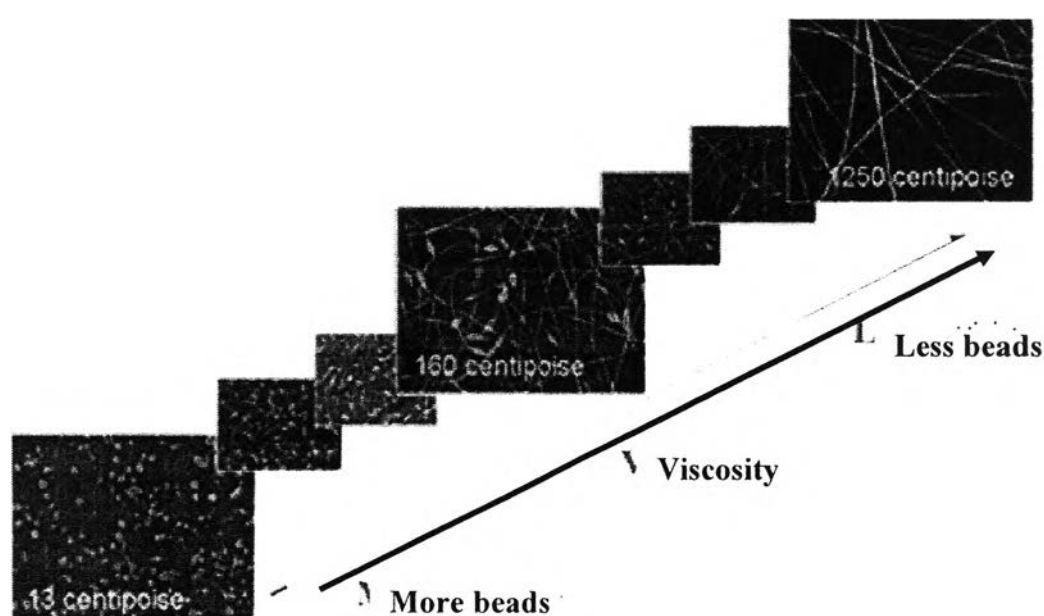
Figure 2.9. SEM micrographs of electrospun nanofibers from different polymer concentration solutions. (Fong and Reneker, 1999).

2.5.2 Fiber Alignment

Teo and Ramakrishna (2006) summarized various designs of the collector for obtaining aligned electrospun fiber. As shown in Table 2.1, several researchers have shown that it is possible to obtain aligned fibers by using a rotating collector (Matthews *et. al* 2002, Kameoka *et. al* 2003, Subramanian *et. al* 2005). Matthews *et. al* demonstrated the effect of the rotating speed of a mandrel on the degree of electrospun collagen fiber alignment. At a speed of less than 500 rpm, a random mix of collagen fibers was collected. However, when the rotating speed of

the mandrel was increased to 4500 rpm (approximately 1.4 ms^{-1} at the surface of the mandrel), the collagen fibers showed significant alignment along the axis of rotation. Mechanical testing of the aligned scaffold showed that the peak stress along the principal fiber alignment was 1.5 ± 0.2 MPa and the average modulus was 52.3 ± 5.2 MPa, while the peak stress across the principal fiber alignment was 0.7 ± 0.1 MPa and the modulus was 26.1 ± 4.0 MPa (Matthews *et. al* 2002).

Kim *et. al* (2004) examined the effect of the linear velocity of the rotating mandrel on the crystallinity, mechanical properties and alignment of electrospun poly(ethylene terephthalate) (PET). Using wide-angle x-ray diffraction, PET electrospun fibers were found to be more amorphous with increasing mandrel rotation. This is probably due to the rapid solidification and collection of the fibers. However, the increased linear velocity of the mandrel induced greater alignment of the PET crystals in the fibers. Although the Young's modulus, yield stress and tensile stress of the mesh along the PET fiber alignment increased with higher mandrel rotation speed and fiber alignment, the same properties tend to decrease above a linear velocity of 30 m min^{-1}. At a linear velocity of 45 m min^{-1}, many fibers were dispersed into the air instead of being deposited on the mandrel (Kim *et. al* 2004). At such a high rotation speed, the velocity of the electrospinning jet may be slower than the linear velocity of the rotating mandrel. Reported average velocity of the electrospinning jet is ranged from 2 m s^{-1} (Kowalewski *et. al* 2005, Sundaray *et. al* 2004) to 186 m s^{-1} (Smit *et. al* 2005). A separate study by Zussman *et. al* using a rotating disc collector demonstrated that at high enough rotation speed, necking of the electrospun fibers was observed (Zussman *et. al* 2003). This may account for the reduced mechanical properties of the PET mesh collected at high speed by Kim *et. al.* Therefore the mandrel rotation speed and fiber orientation have a direct influence on the material properties of the engineered matrix. The presence of the disoriented fibers collected on the rotating mandrel may be the result of residual charge accumulation on the deposited fibers, which interferes with the alignment of incoming fibers. To achieve greater fiber alignment, a possible way is to reduce the chaotic path of the electrospinning jet and to reduce the residual charge accumulation on the rotating mandrel. Kessick *et. al* used an alternating-current (AC) high voltage

supply instead of a typically used direct-current (DC) high voltage supply to charge the solution for electrospinning. Polyethylene oxide (PEO) collected on a rotating mandrel showed greater degree of fiber alignment using an AC potential than a DC potential. Using an AC potential to charge the solution may have a dual function. The electrospinning jet from an AC potential may consist of short segments of alternating polarity and this may significantly reduce the chaotic path of the electrospinning jet. This allows the fibers to be wound onto the rotating mandrel with greater ease and alignment. Given the presence of both positive and negative charges on the surface of the rotating mandrel, there will be a neutralizing effect over the area of the mesh, thus minimizing charge accumulation (Kessick *et. al* 2004).

Table 2.1 Schematic diagram of various electrospinning set-ups for multiple spinnerets and to obtain various fibrous assemblies (Teo and Ramakrishna 2006)
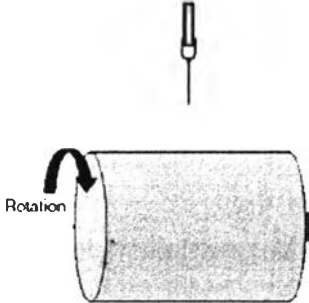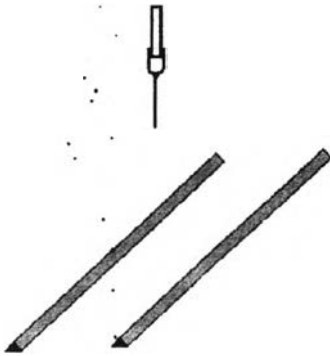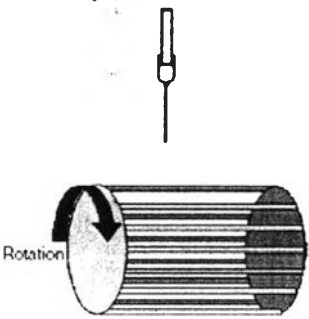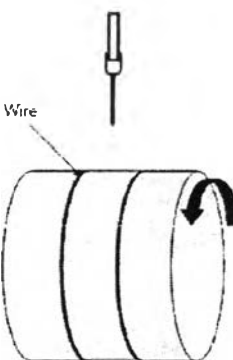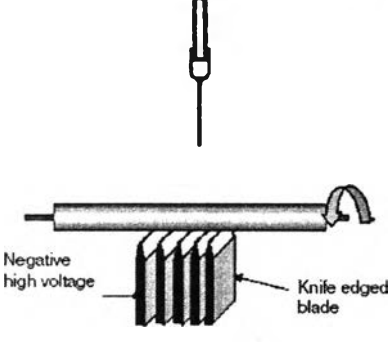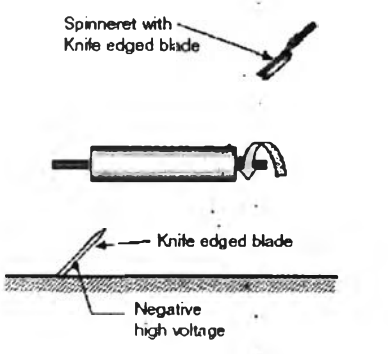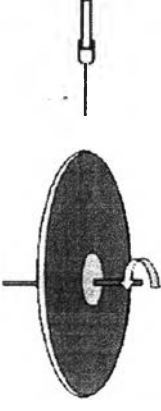
	Assembly-aligned fibrous mesh
A. Rotating drum Rotation	**Advantage** Simple set-up Large area of aligned fibres can be fabricated **Disadvantage** Highly aligned fibrous assemblies are difficult to fabricate Fibre breakage may occur if rotating speed is too high (Matthews et al 2002, Kim et al 2004, Chew et al 2005, Wannatong et al 2004)
B. Parallel electrodes	**Advantage** Simple set-up Highly aligned fibres are easy to obtain Aligned fibres are easily transferable to another substrate **Disadvantage** Thicker layer of aligned fibres are not possible There is a limit in the length of the aligned fibres (Li et al 2003)
C. Rotating wire drum collector Rotation	**Advantage** Simple set-up Highly aligned fibres are possible **Disadvantage** Thicker layer of aligned fibres are not possible Fibres may not be aligned throughout the whole assembly (Katta et al 2004)
D. Drum collector with wire wound on it Wire	**Advantage** Simple set-up Highly aligned fibres are possible Area of aligned fibres on the wire is adjustable by varying wire thickness **Disadvantage** Aligned fibres are concentrated on the wire instead of the whole drum (Bhattarai et al 2005)

Table 2.1. (Continued.)

E. Rotating tube collector with knife-edge electrodes below 	**Advantage** Highly aligned fibres possible Aligned fibres covered the whole tube Thicker layer of aligned fibre deposition is possible **Disadvantage** Set-up requires a negative electrode to be effective Only possible for small diameter tube (Teo *et al* 2005)
F. Controlling electrospinning jet using knife-edge electrodes 	**Advantage** Highly aligned fibres possible Able to control the direction of fibre alignment on the tube Thicker layer of aligned fibre deposition is possible **Disadvantage** Set-up requires a negative electrode to be effective Only possible for small diameter tube (Teo *et al* 2005)
G. Disc collector 	**Advantage** Simple set-up Highly aligned fibres are possible Able to fabricate arrayed fibres by attaching a rotatable table on the edge of the disc **Disadvantage** Unable to retain high fibre alignment at the same rotating speed when the deposited fibres are thicker Small area of fibre alignment (Theron *et al* 2001, Inai *et al* 2005, Xu *et al* 2004)

2.6 Points of the Present Work

The present work focuses on developing of polyoxymethylene (POM) for novel nanomaterials. As the approaches to develop the POM nanomaterials can be either from the incorporation of the appropriate additives to achieve the improvement of the POM properties or the fabrication to create novel materials for the use in advanced applications, the present work covers both approaches.

In the first part (Chapter 3), the work concentrates on how we can achieve polyoxymethylene/bentonite based nanocomposite and what factors affect to the structure and properties of the materials obtained. The work shows the role of the primary ammonium surfactant treated bentonite in the formation of the exfoliated POM nanocomposites.

In the second part (Chapters 4 and 5); the work demonstrates the way to obtain electrospun POM nanofibers via the electrospinning process using a hexafluoroisopropanol (HFIP)-based solvent system. The fundamental aspect for achieving the electrospun POM nanofibers with specific surface properties is clarified. The work also clarifies the structural changes of the electrospun POM nanofiber as an effect of the electrospinning process.